

Figure 1.1 Components of the TOA radiation budget for the Earth and its atmosphere.

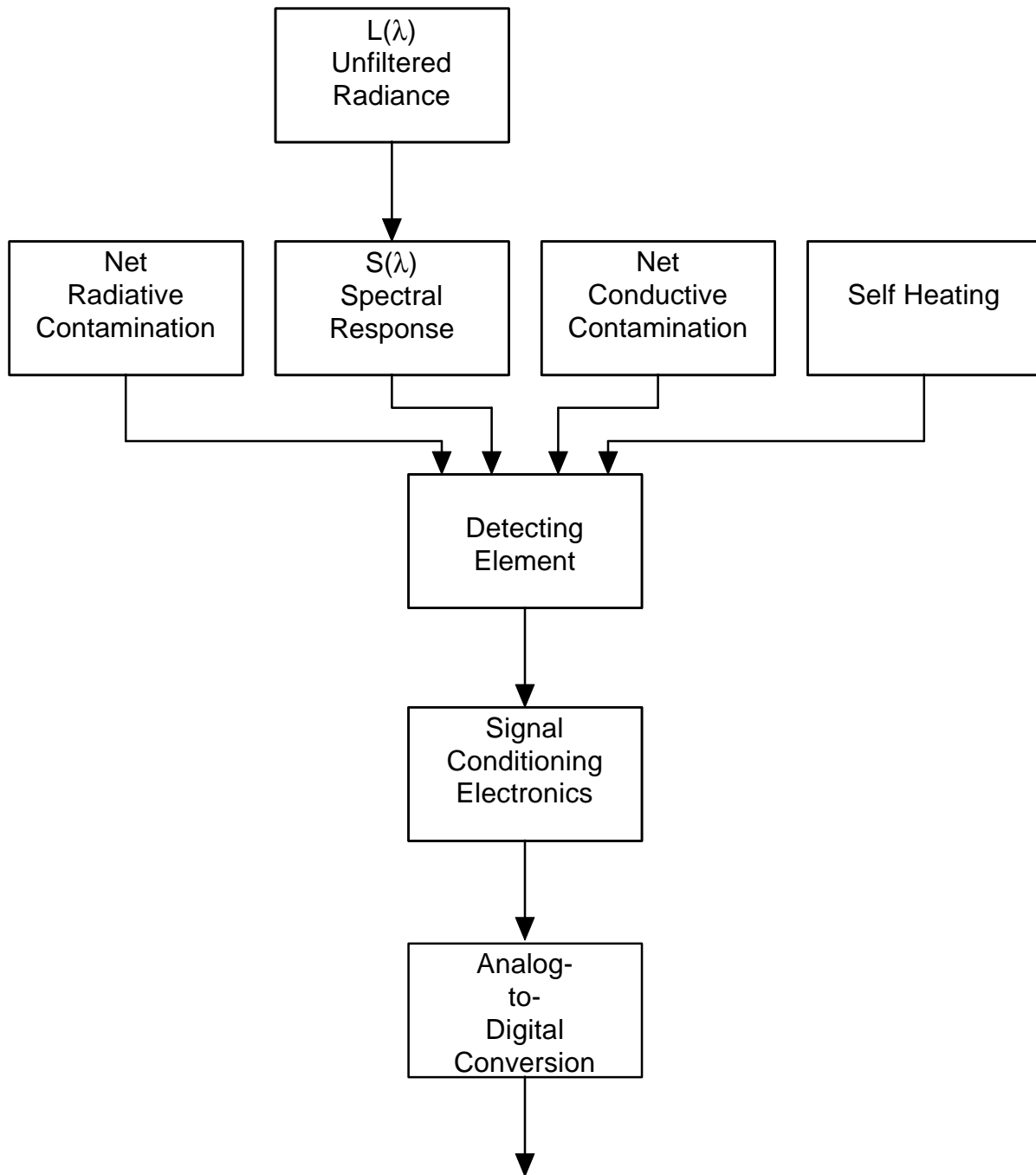


Figure 2.1 Components of a general radiometric system.

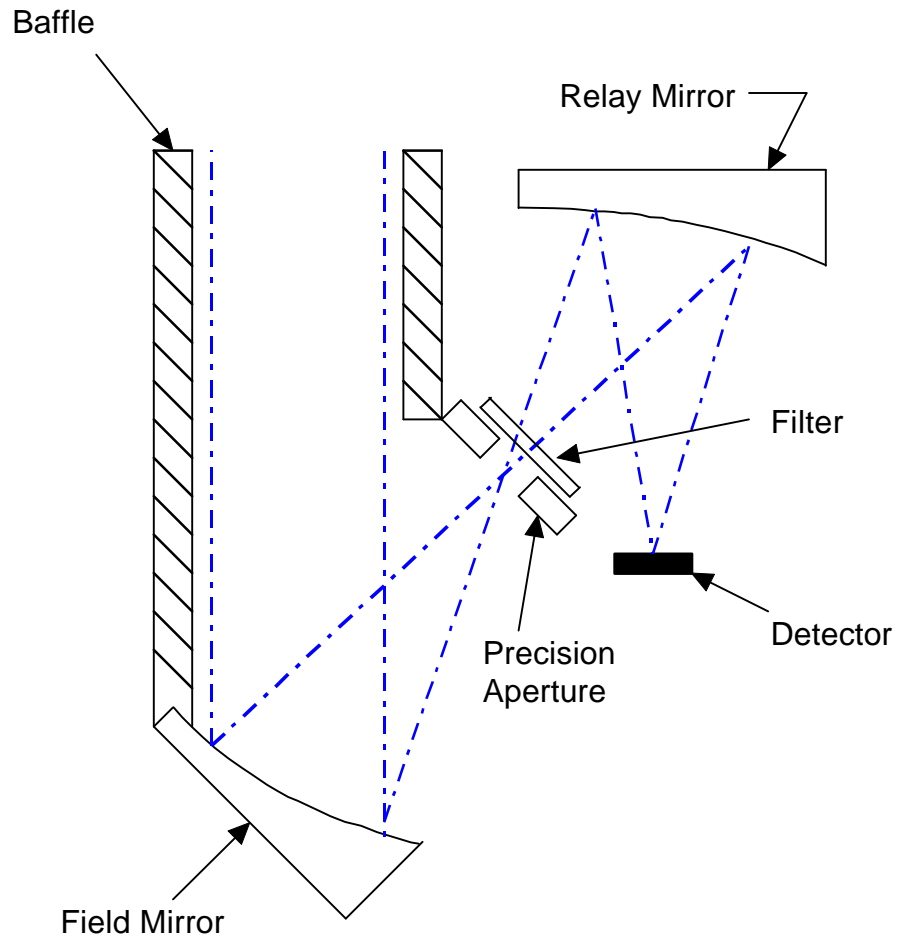


Figure 2.2 Off-axis optical system.

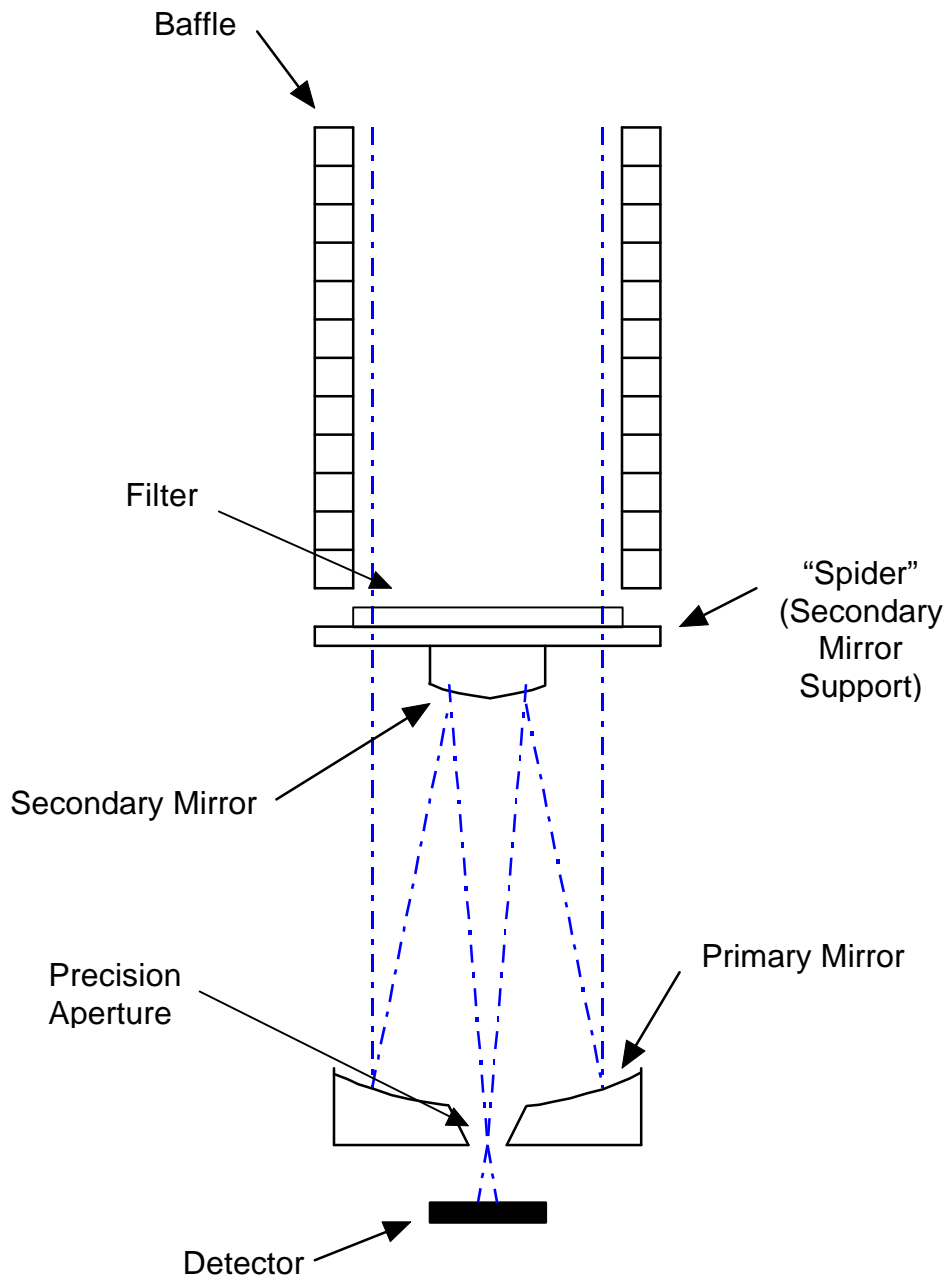


Figure 2.3 Cassegrain optical system.

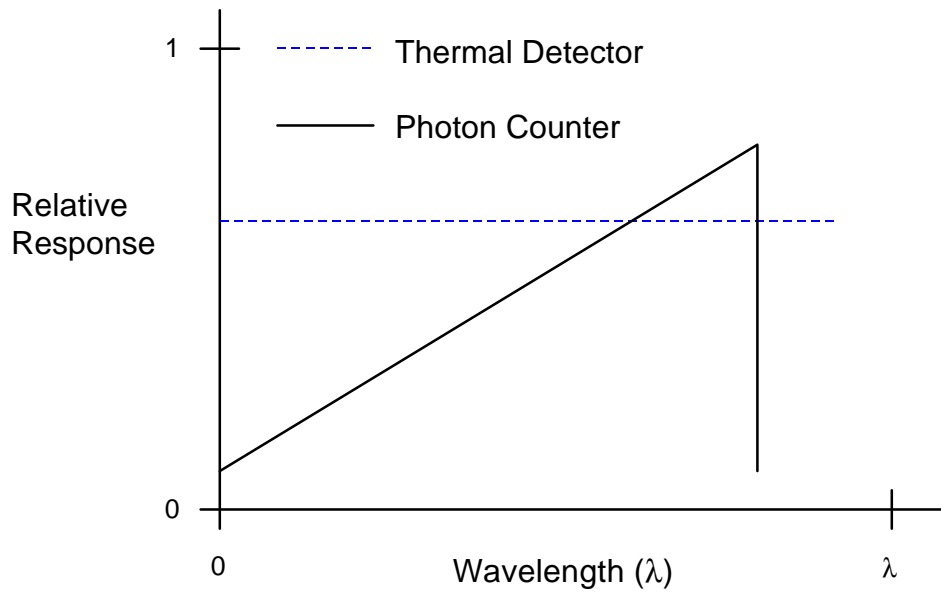


Figure 2.4 Ideal behavior of thermal detectors and photon counters.

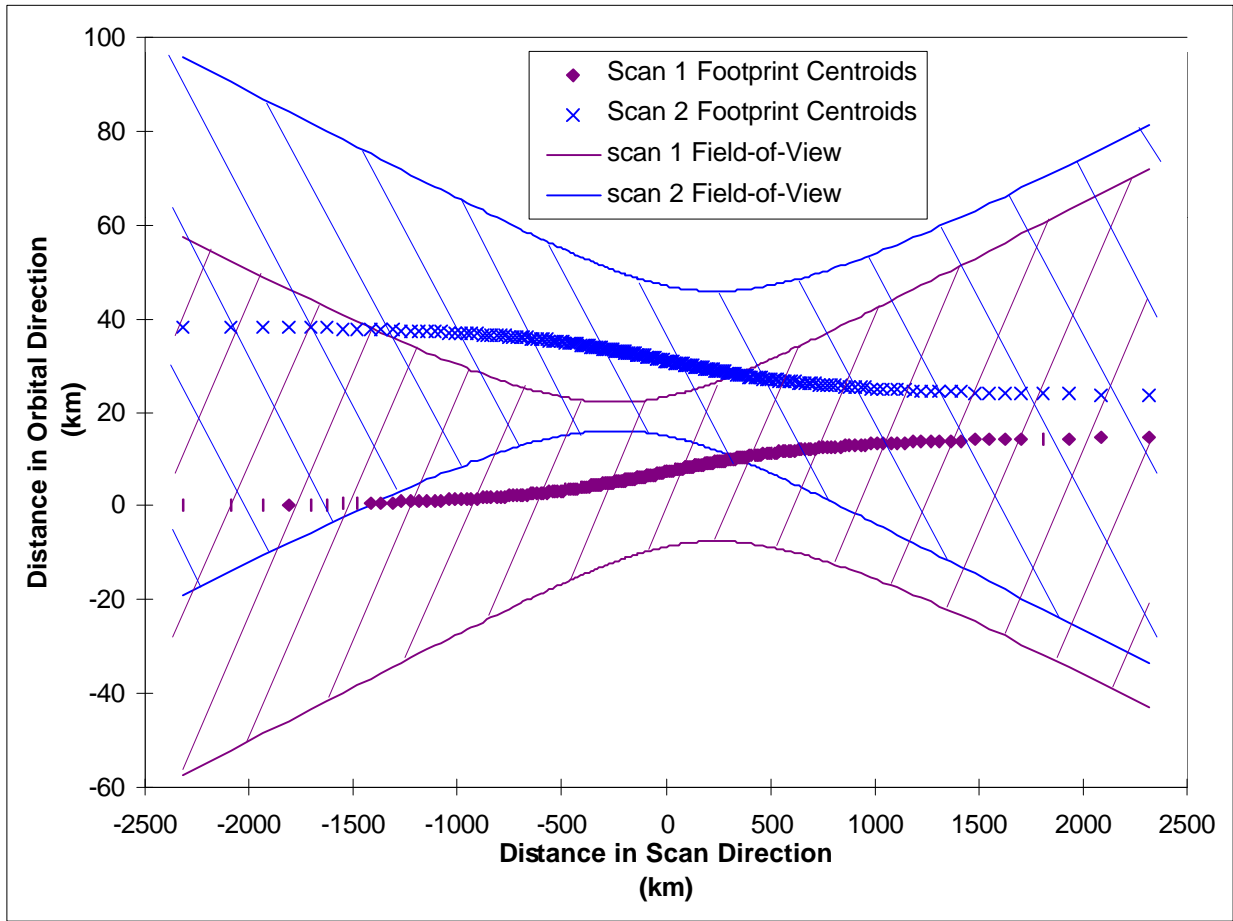


Figure 2.5. Illustration of overlap in instantaneous footprints for an instrument which scans perpendicular to the orbital direction.

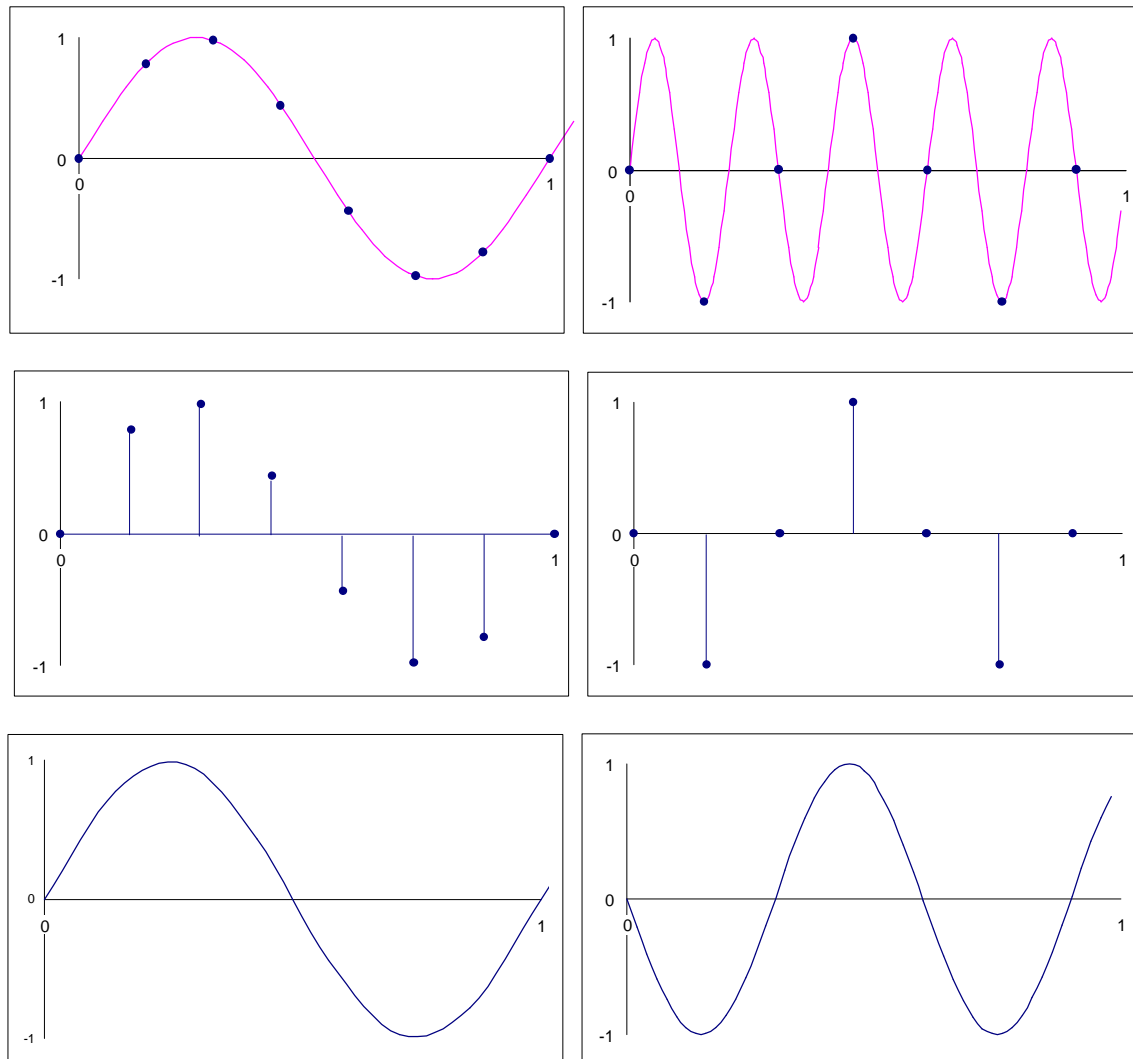


Figure 2.6 Illustration of aliasing error. On the left, the sampling frequency is seven times the original frequency; while on the right, the sampling frequency is  $7/5$  of the original frequency [39].

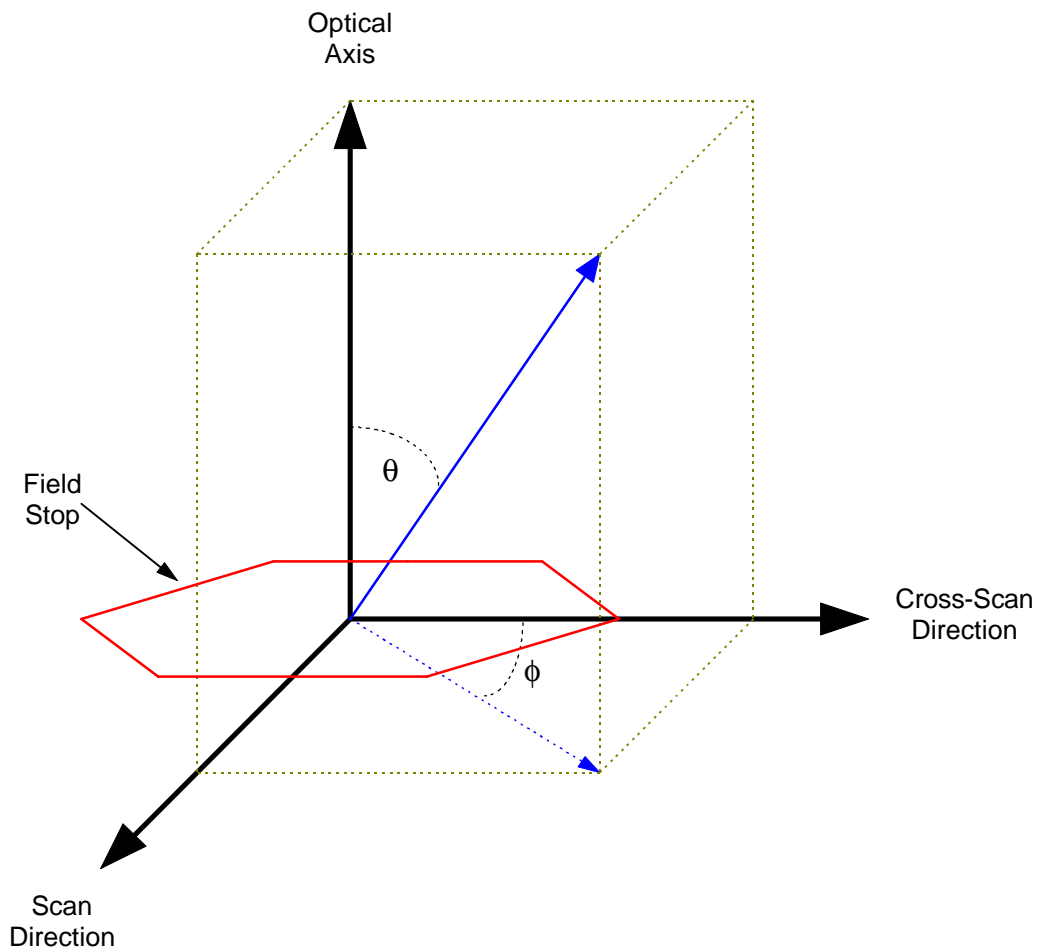


Figure 2.7 Illustration of zenith,  $\theta$ , and azimuth,  $\phi$ , angles used to define the instrument field-of-view.



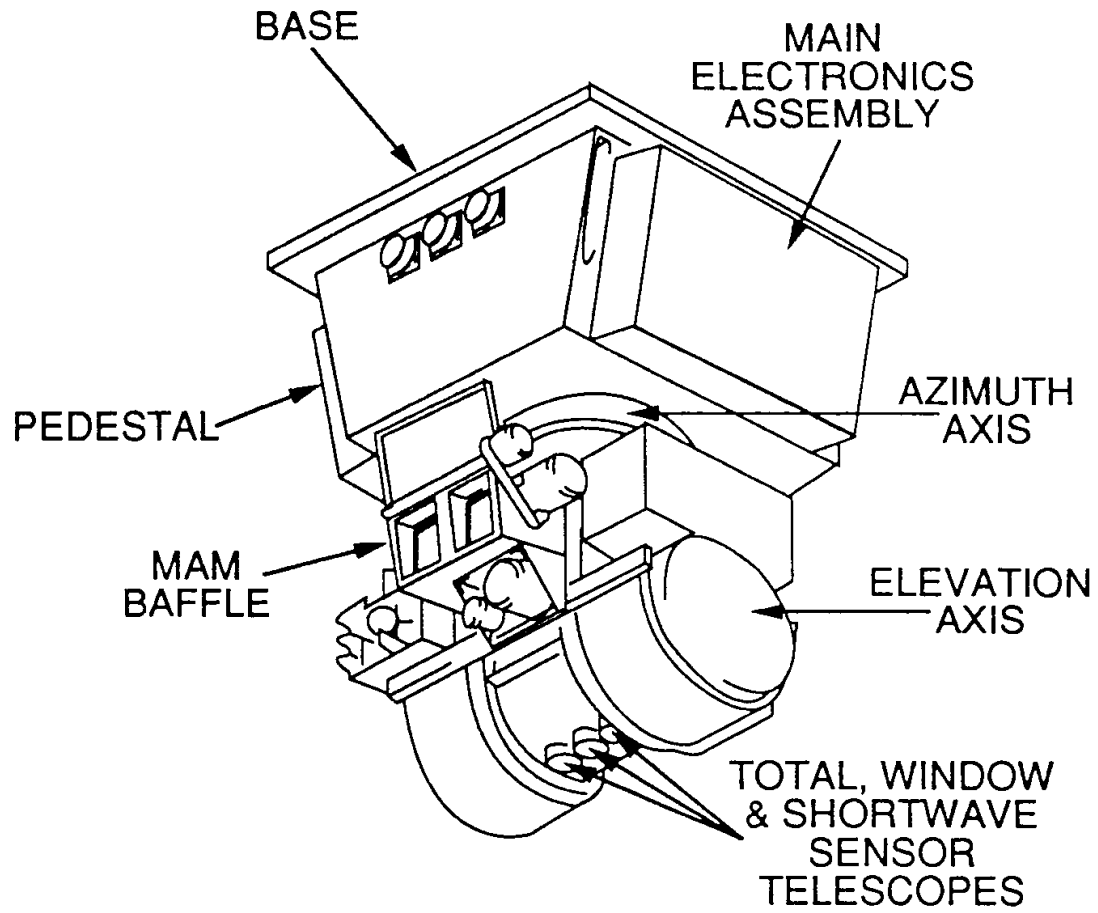


Figure 3.1 CERES instrument package.

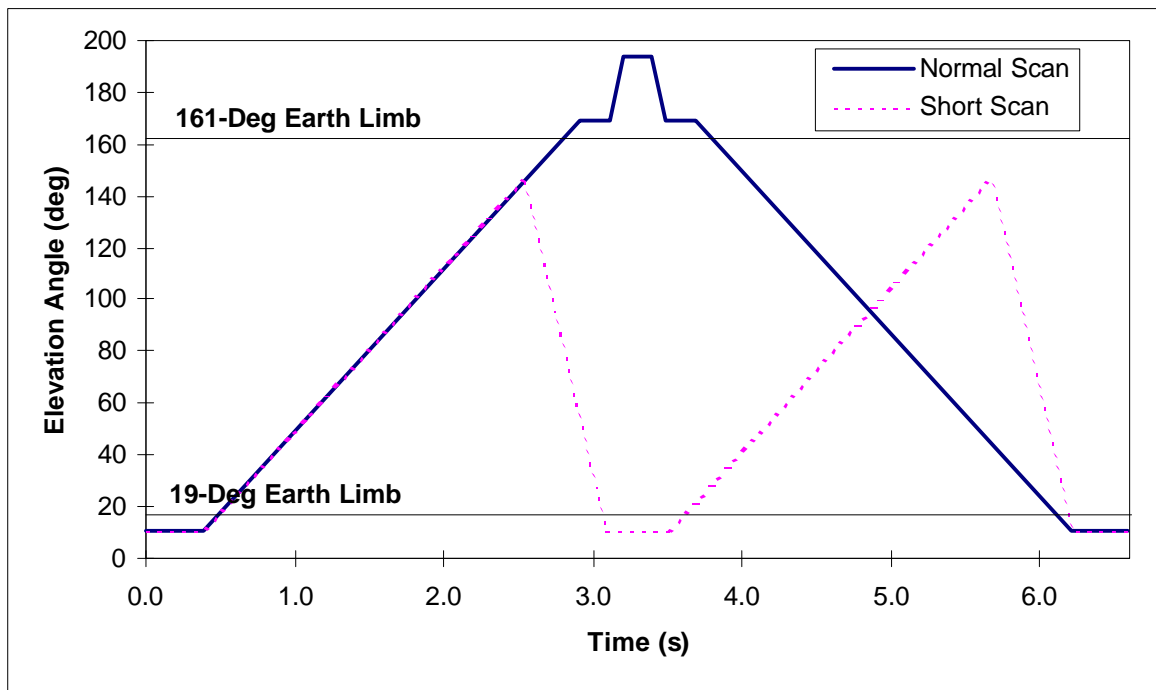


Figure 3.2 Elevation scan profiles for the CERES Proto-Flight Model (PFM) located on the Tropical Rainfall Measuring Mission (TRMM) spacecraft.

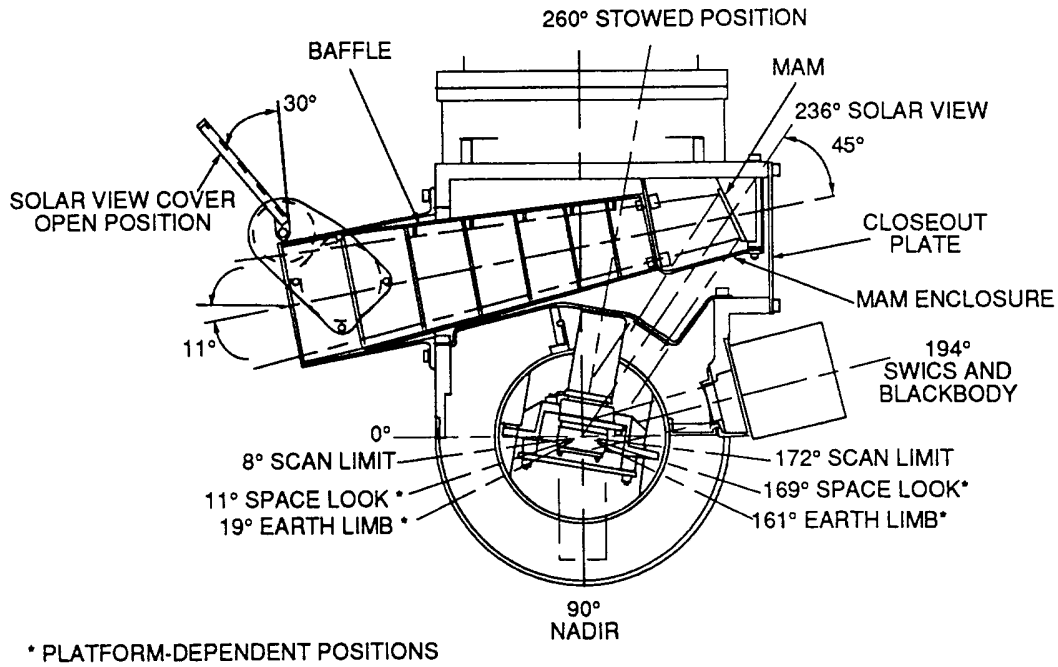
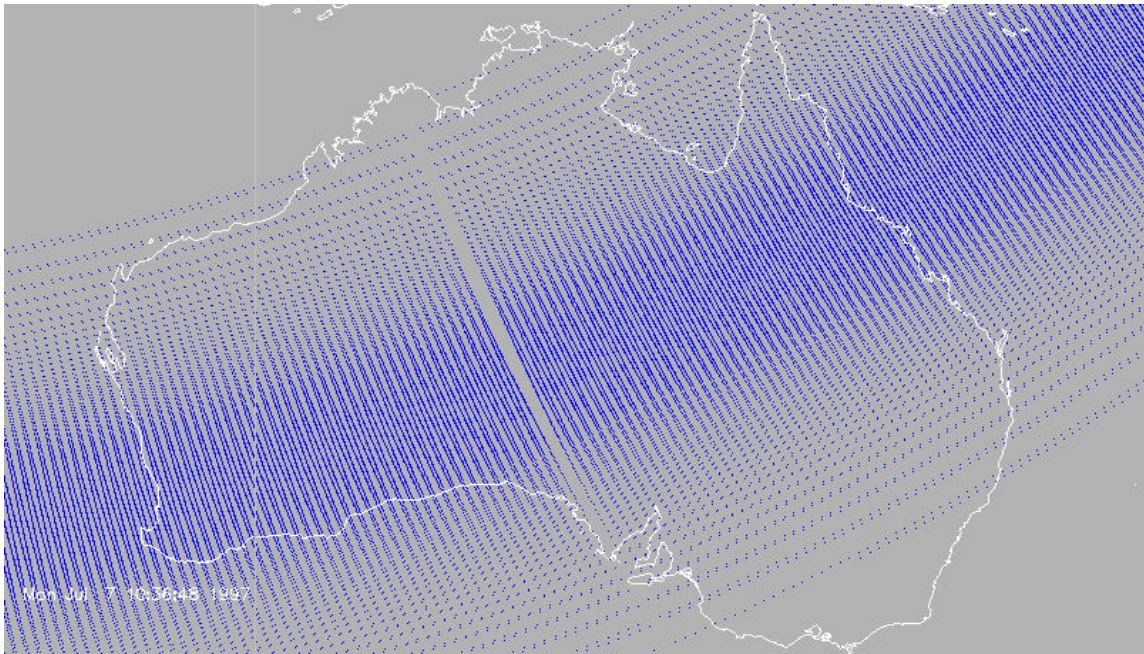
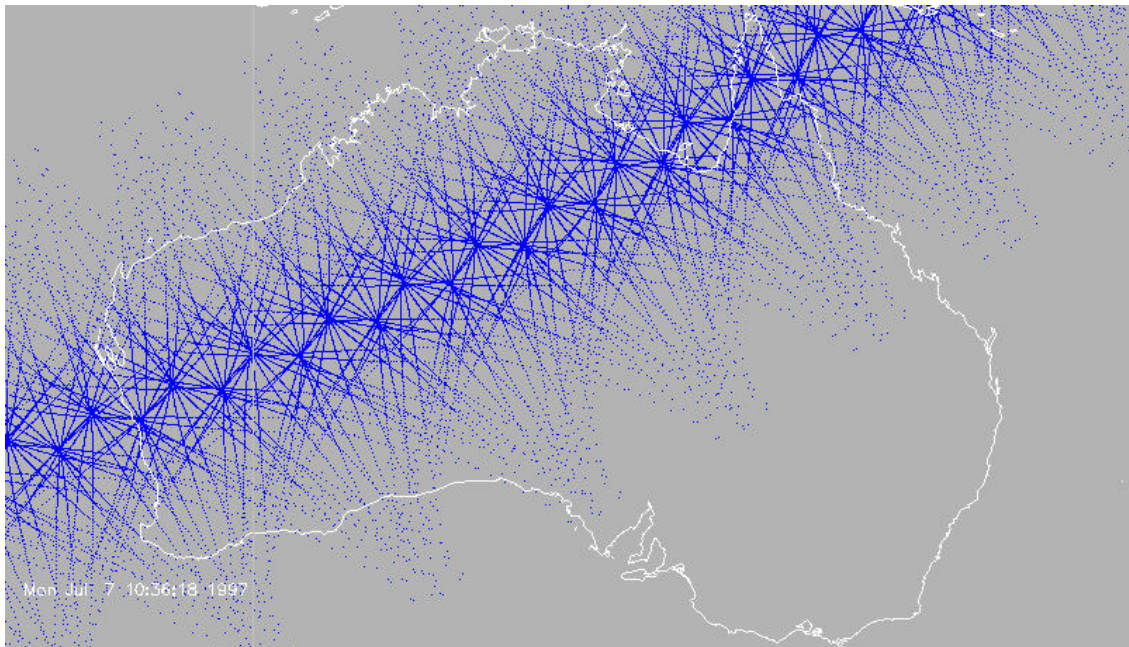


Figure 3.3 Cross-sectional view of a CERES instrument.



(a)



(b)

Figure 3.4 Illustration of footprint scan patterns for (a) normal cross-track scan mode, and (b) biaxial scan mode.

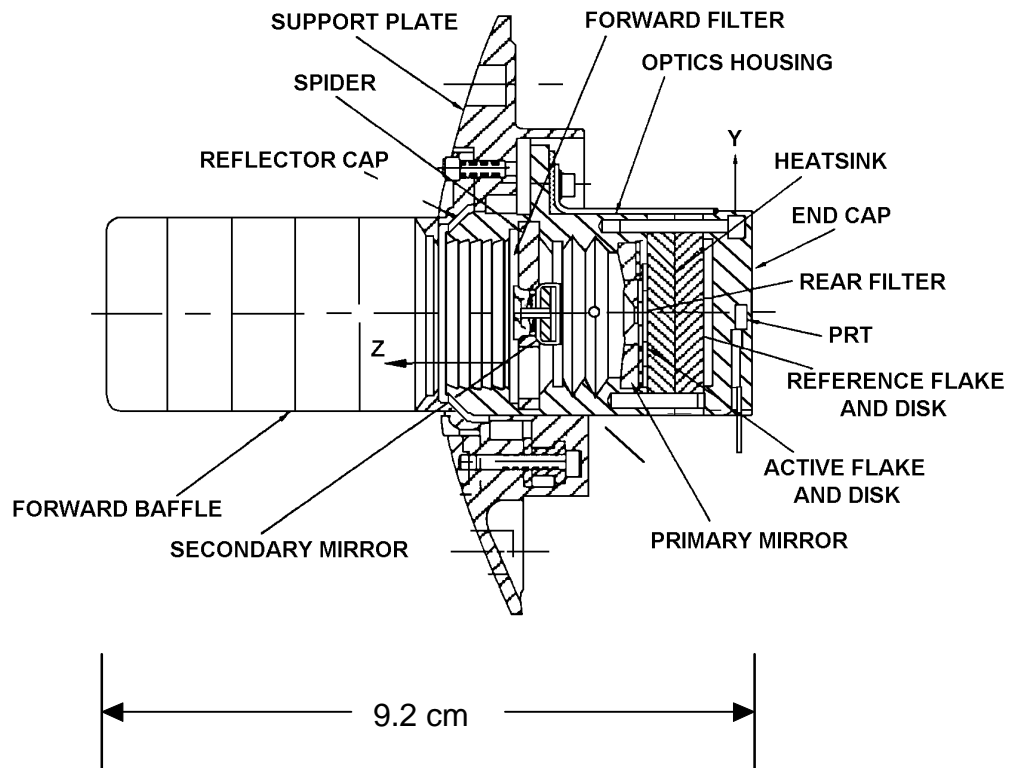


Figure 3.5 A CERES radiometric channel.

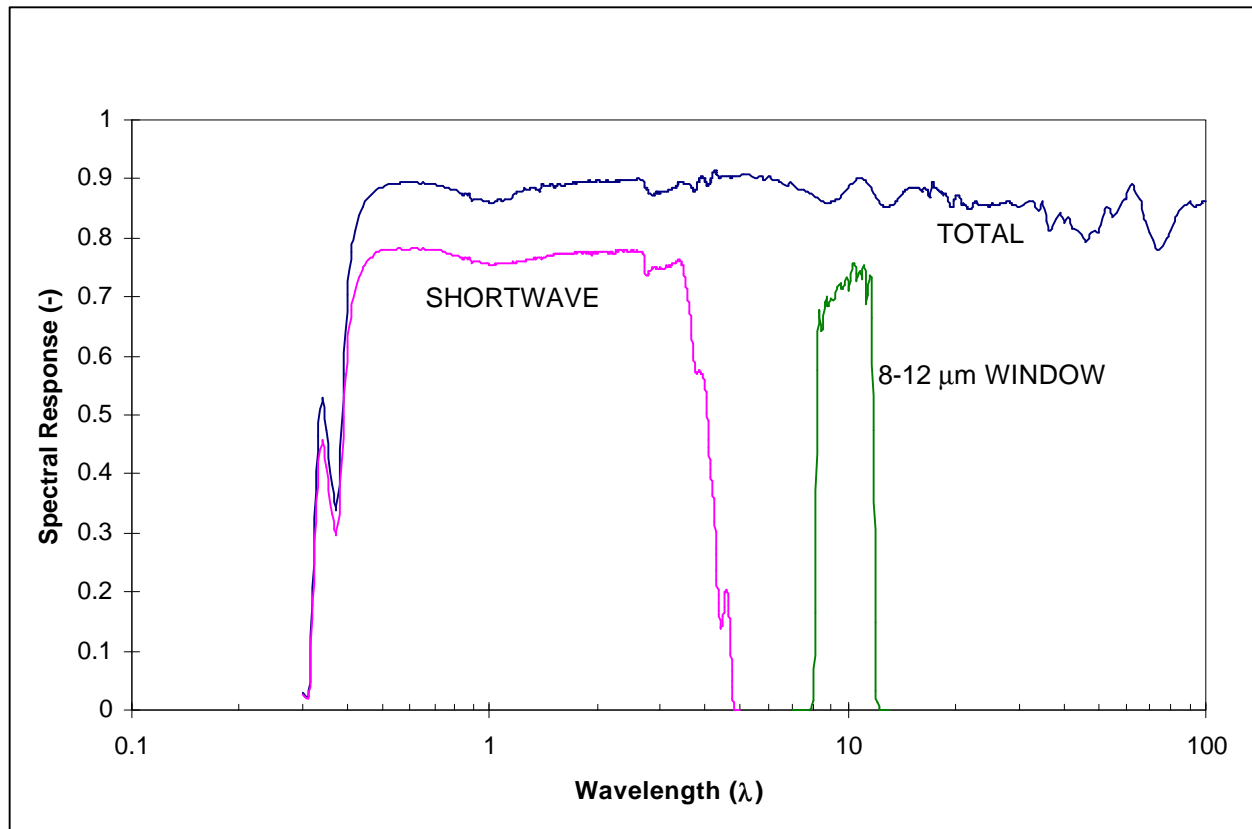


Figure 3.6 End-to-end spectral response for the CERES PFM radiometric channels.

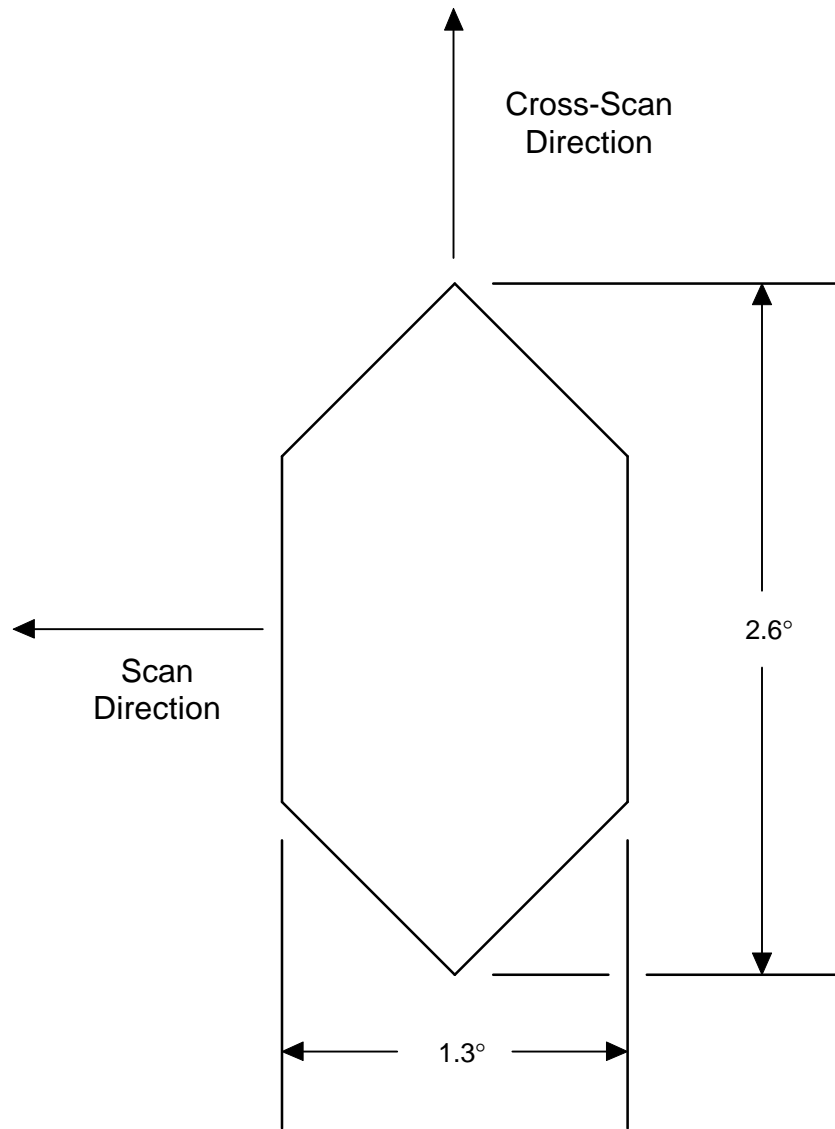


Figure 3.7 Truncated diamond precision aperture for the CERES radiometric channels.

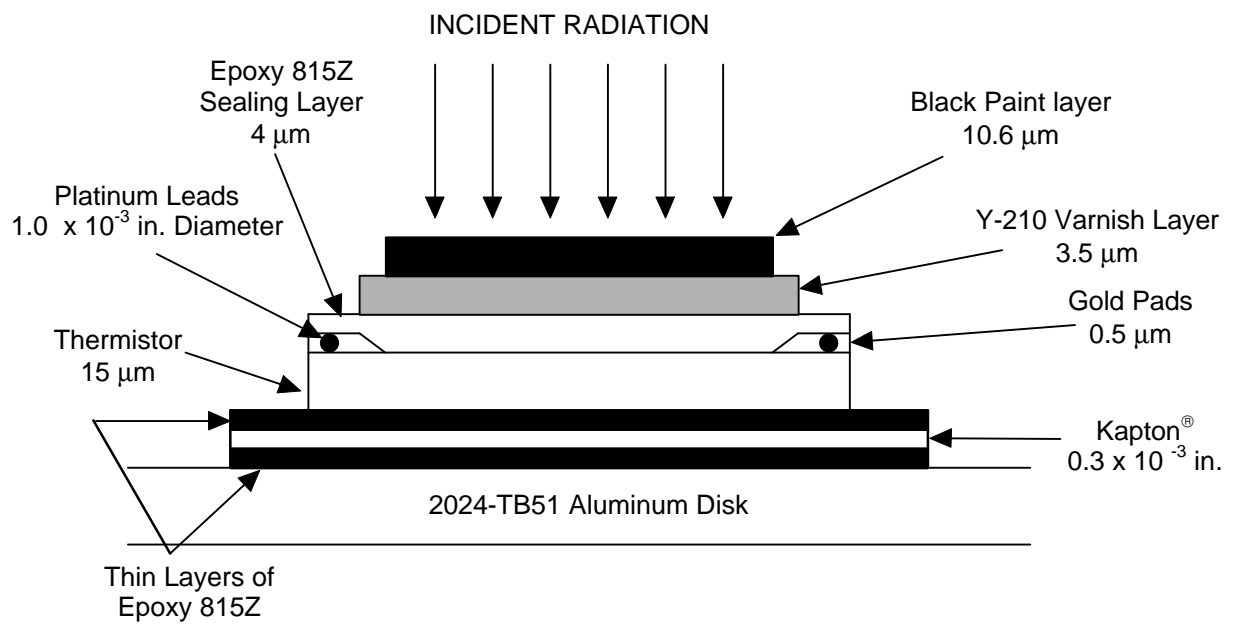


Figure 3.8 CERES Proto-Flight Model detector nominal specifications.



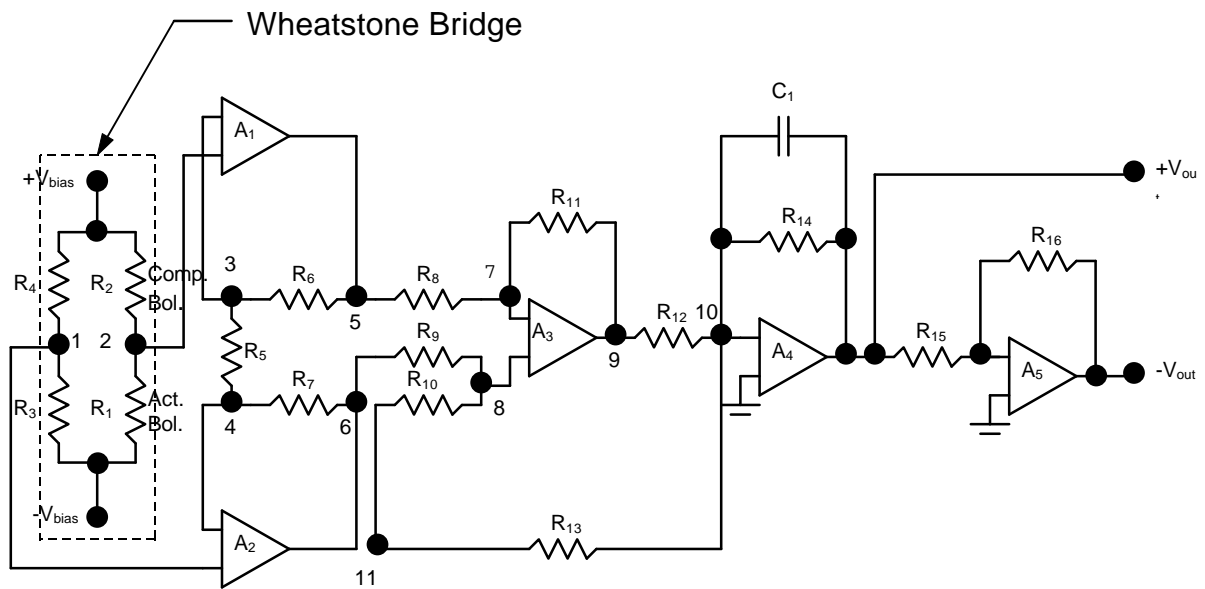


Figure 3.9 CERES Proto-Flight Model pre-amplifier electronic circuit.

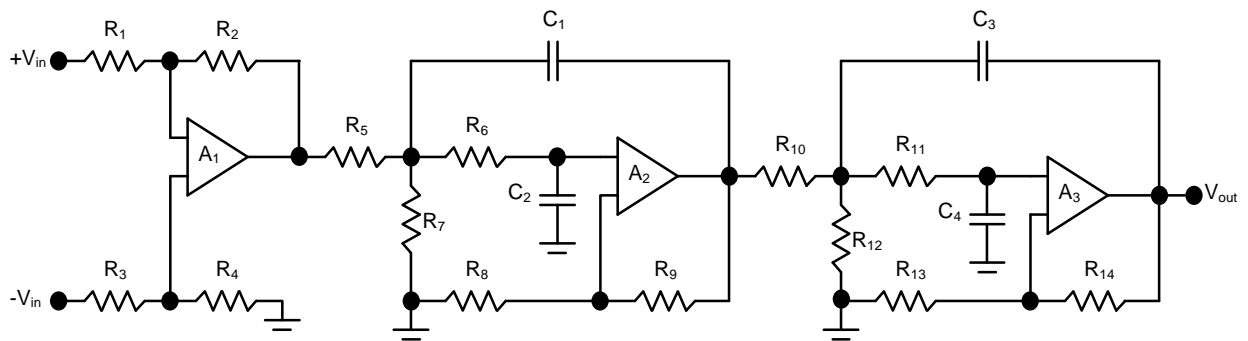


Figure 3.10 CERES Four-pole Bessel filter.

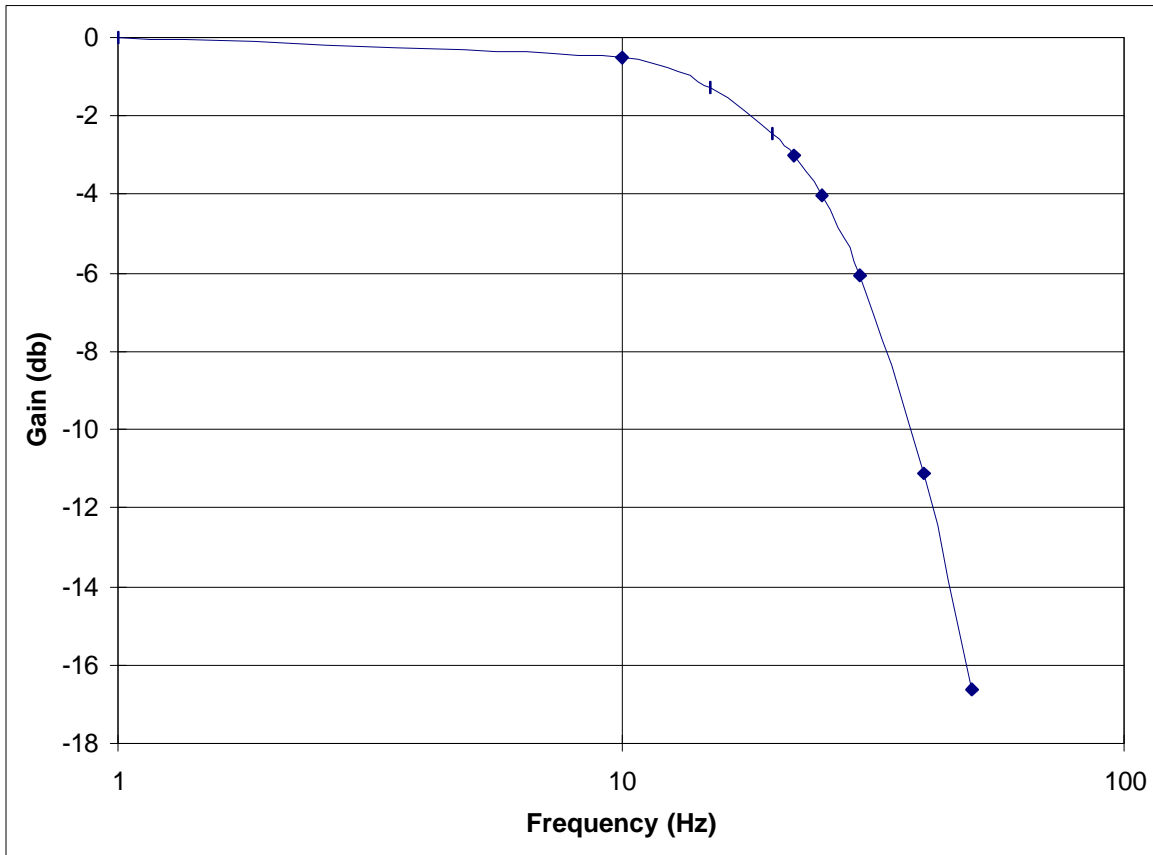


Figure 3.11 Computed bode diagram for the CERES 4-pole Bessel filter.

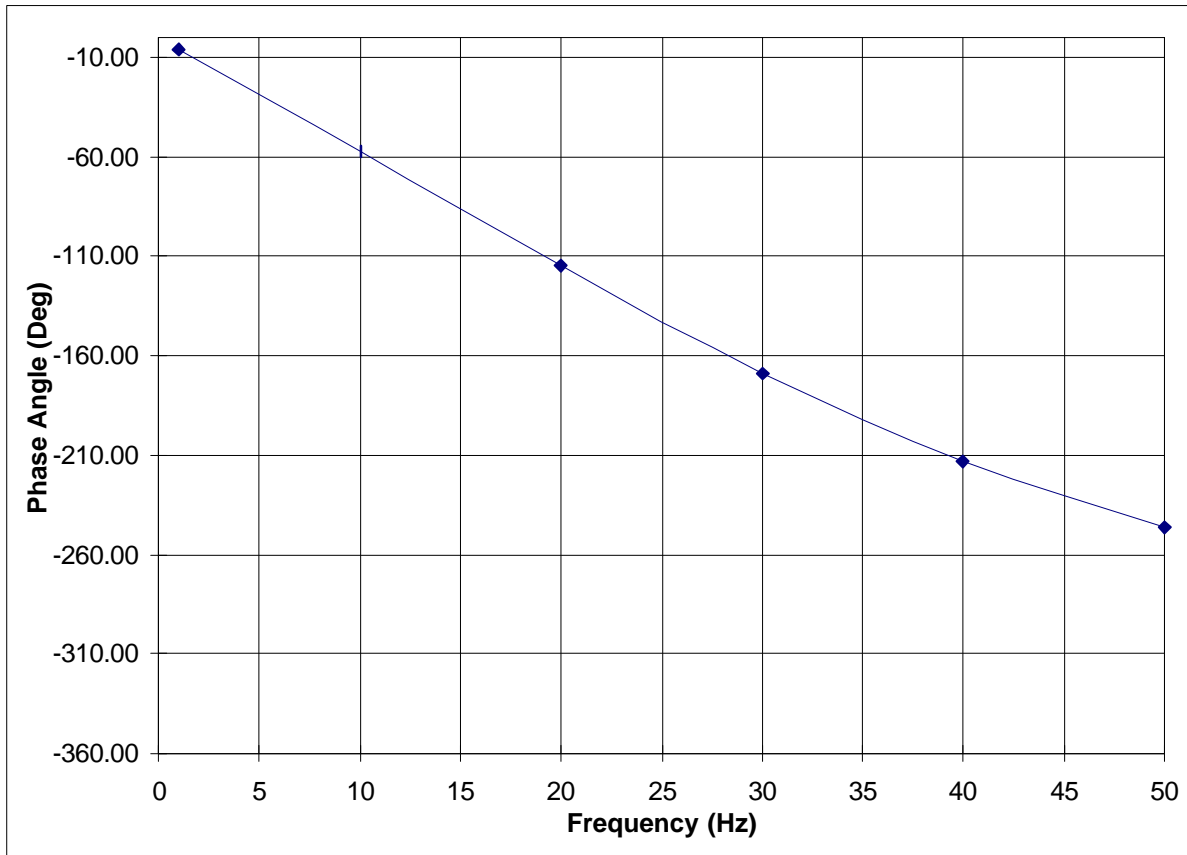


Figure 3.12 Computed phase angle diagram for the CERES four-pole Bessel filter.

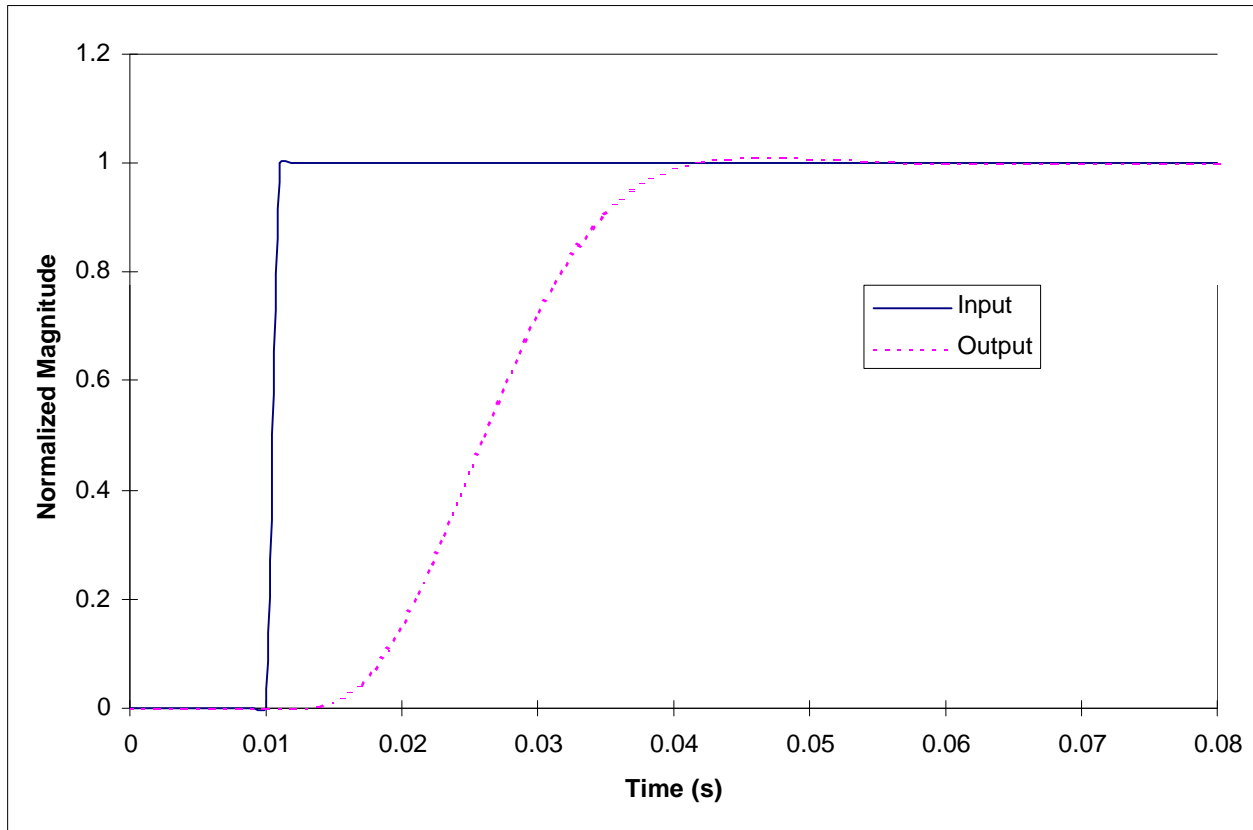


Figure 3.13 Filtering function for the CERES 4-pole Bessel filter.

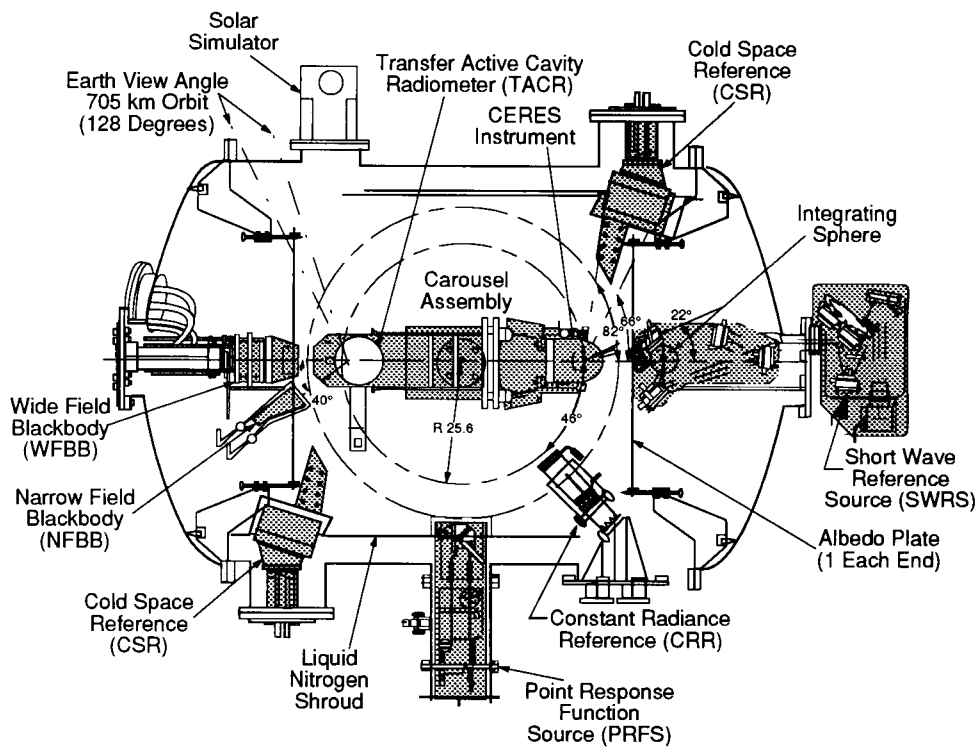


Figure 3.14 TRW's Radiometric Calibration Facility (RCF) used in the CERES ground calibration [18].

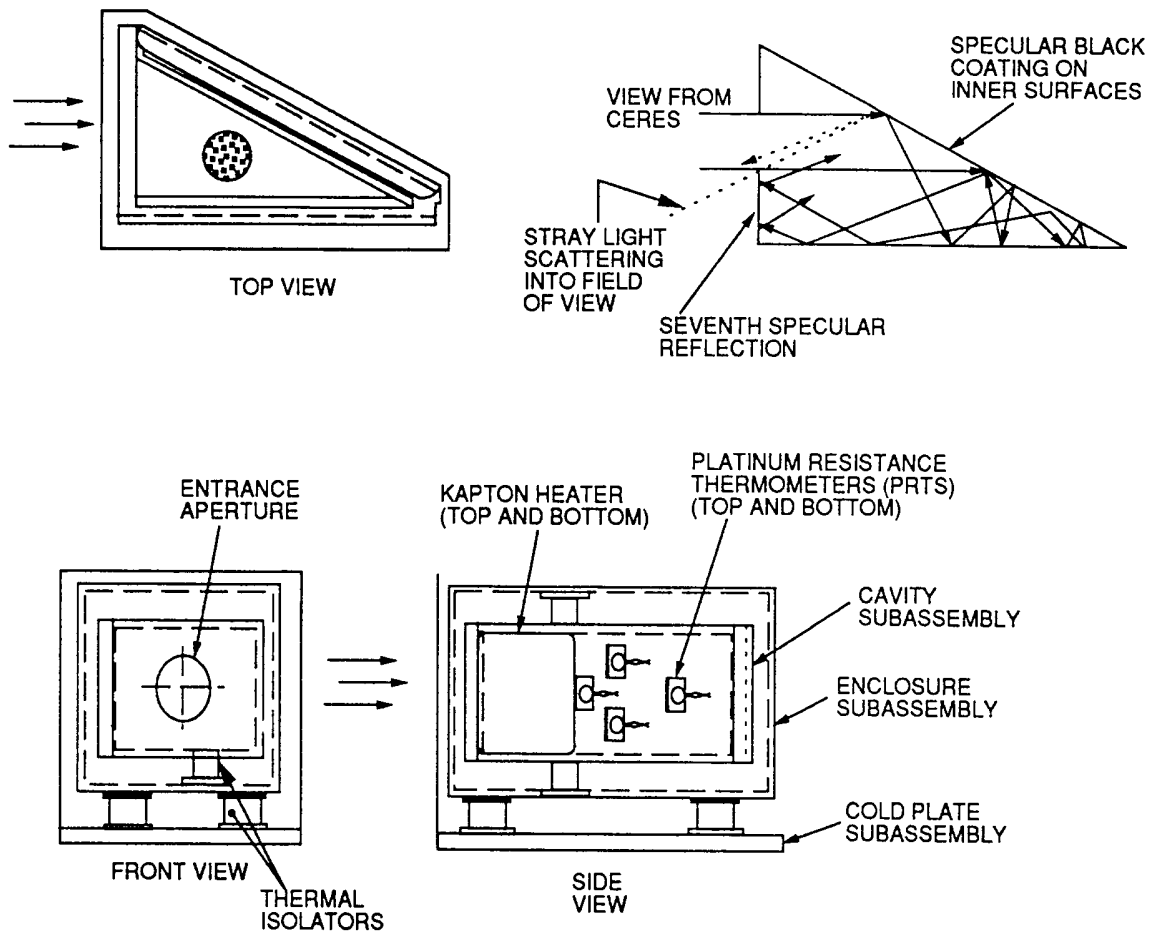


Figure 3.15 Narrow Field Black Body (NFBB) used in the CERES Radiometric Calibration Facility (RCF) [18].

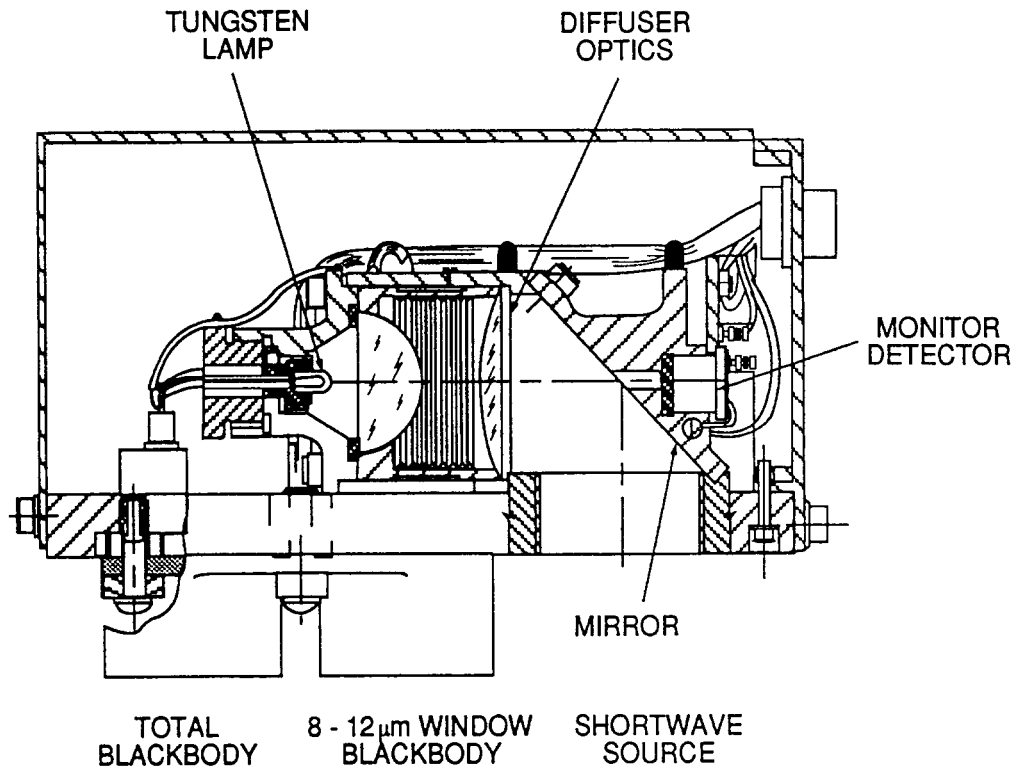


Figure 3.16 CERES Internal Calibration Source (ICS) module [18].



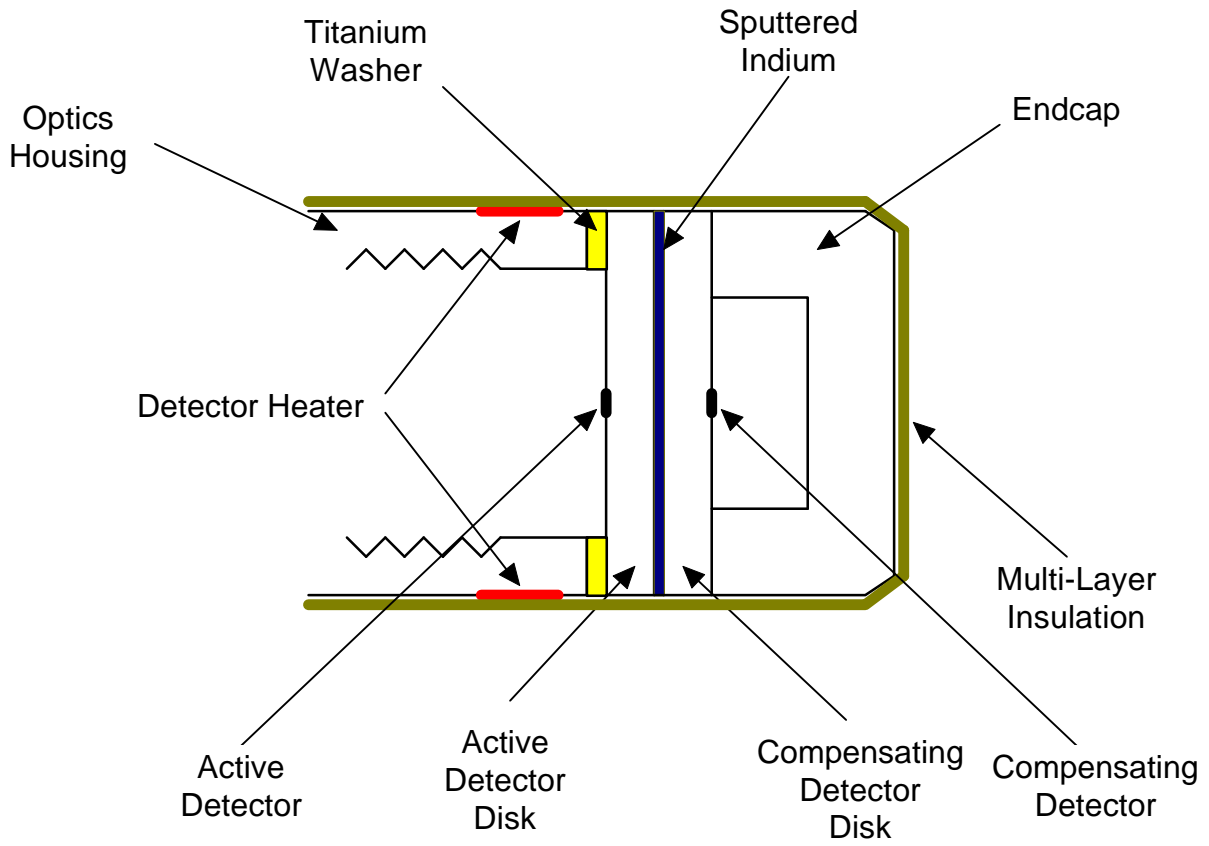


Figure 4.1 Schematic of the Detector Module Assembly (Not To Scale).

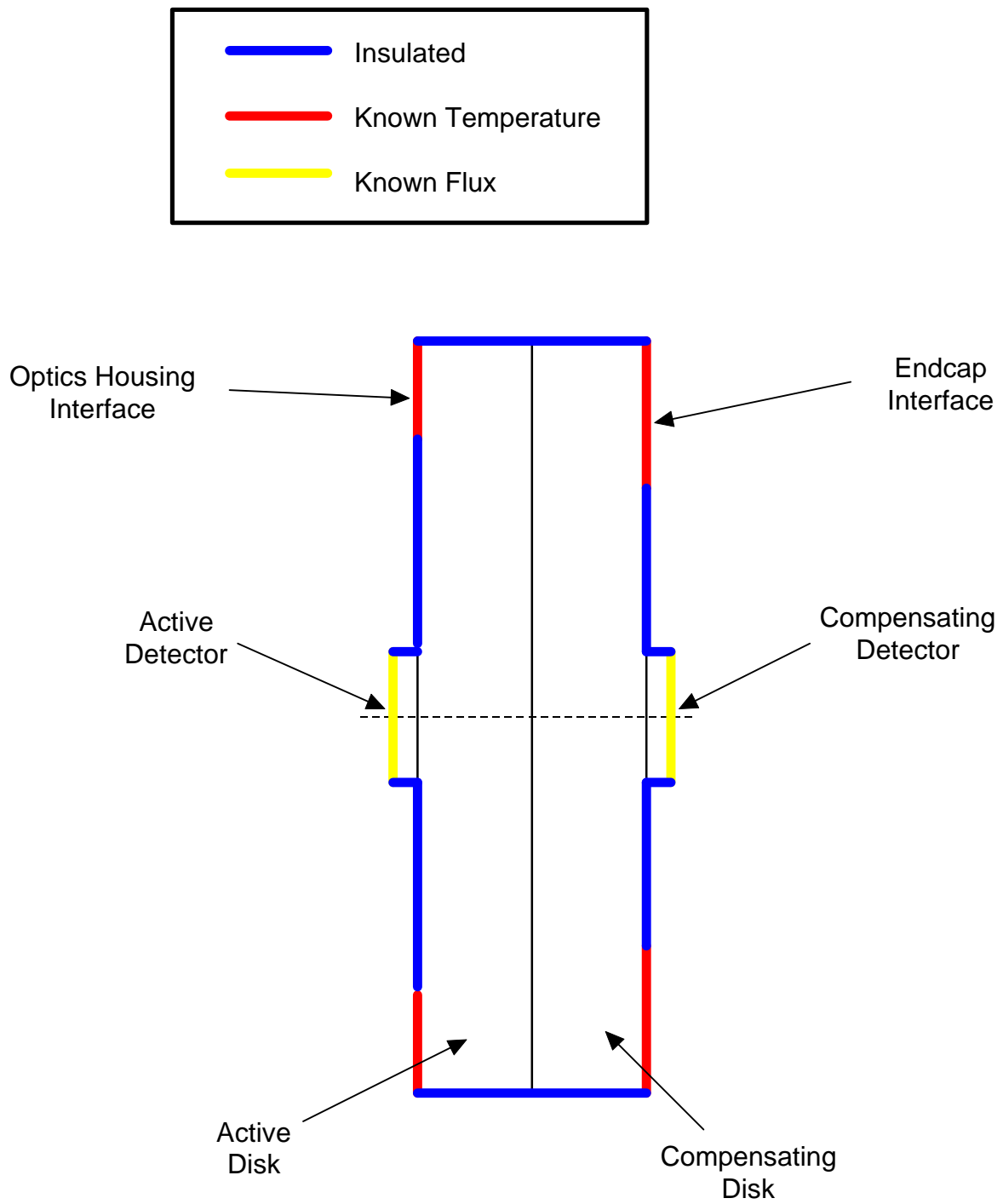


Figure 4.2 Illustration of the modeled boundary conditions.